surface composition and not necessarily respond to the Fermi levels.

In conclusion, a relationship with the Hammett σ is not a proof of electron transfer. For the present case the results are better explained in terms of ion transfer, most likely proton transfer. This mechanism is particularly favored considering the amount of energy required to detach electrons in ambient conditions. The change in the sign of the charge within a series can in principle result from a change in the direction of proton transfer when there is a shift in the relative basicities of two closely matched materials. This sign change is difficult to explain in terms of changes in the relative donor/acceptor energy levels. Thus, there is no need to invoke the electron-transfer mechanism, even though it cannot be ruled out. In concurrence with Kornfield,[8] we believe that ions transfer between two surfaces, and the direction and amount of transfer will depend on the relative basicity and "ion affinities" of the surfaces. Finally, we find that these aniline and anil derivatives are not appropriate for studying charging mechanisms because of the large amount of material transfer between the two surfaces.

Acknowledgment. We thank Jose Vazquez and David Dreblow for their technical assistance with certain aspects of this study. J.G. is grateful to the Natural Sciences and Engineering Research Council of Canada for a postdoctoral fellowship.

Registry No. SAL-H, 779-84-0; SAL-OCH_3, 889-08-7; BEN-OCH_3, 783-08-4; BEN-H, 538-51-2; AN-NO_2, 100-01-6; AN-CH_3, 106-49-0; AN-OCH_3, 104-94-9; AN-NH_2, 106-50-3; Fe, 7439-89-6.

(45) Homewood, K. P. *J. Phys. D: Appl. Phys.* **1984**, *17*, 1255.

Characterization of Copper(II)-Substituted Synthetic Fluorohectorite Clay and Interaction with Adsorbates by Electron Spin Resonance, Electron Spin Echo Modulation, and Infrared Spectroscopies

Vittorio Luca, Xinhua Chen, and Larry Kevan*

Department of Chemistry, University of Houston, Houston, Texas 77204-5641

Received May 24, 1991. Revised Manuscript Received September 16, 1991

Fluorohectorite containing lattice Cu(II) is synthesized and characterized by electron spin resonance (ESR) and electron spin echo modulation (ESEM) spectroscopies. Three Cu(II) species are identified in the ESR spectrum of this Cu(II)-substituted fluorohectorite. Species A and B have hyperfine splitting constants of 118×10^{-4} and 50×10^{-4} cm^{-1}, respectively, while species C gives spectra that are not well resolved from the $g_\perp$ region of species A and B. On the basis of ESEM measurements, species B is assigned to Cu(II) in octahedral sites with Li(I) in a neighboring octahedral site and species A is assigned to Cu(II) in octahedral sites with no Li(I) in a neighboring octahedral site. Species C is assigned to coordinatively unsaturated Cu(II) sites that are part of the octahedral sheet but that are at the termination of the crystallites, i.e., edge lattice sites. At activation temperatures of 400 °C, species C sites interact strongly with Lewis bases such as pyridine and ammonia. Infrared measurements show that species C sites have moderate Lewis acid strength and also apparently coordinate water molecules but not benzene.

Introduction

The strength of interaction between an adsorbate molecule possessing functional groups such as O or N and metal ions imbedded in a host lattice depends on the electron-donating capability of the adsorbate molecule and the electron-accepting capability of the metal ion (Lewis acid). The transition metals with partially occupied d orbitals possess relatively strong coordinating properties (i.e., they are strong Lewis acids). It is the Lewis acid strength of the transition-metal ions which controls their catalytic activity. The Lewis acid strength depends not only on the nature of the metal ion but also on the interaction of the metal with the substrate.

Clay minerals possess a melange of surface-active sites.[1] Here we focus on transition-metal-ion sites in smectite clays. These can be divided into ion-exchange sites in the interlayer space and lattice sites within the clay structure. In smectite clays there are both octahedrally and tetrahedrally coordinated sites in the clay layer. In nature, smectite clay minerals are found that contain a variety of transition-metal ions in lattice sites. For instance Cr(III), V(III), Ti(III), and Mn(II) are found substituting to various extents in octahedral sites for the more common lattice ions such as Si(IV), Al(III), Fe(III), Fe(II), and Mg(II).[2-4]

Laszlo and Mathy[5] have shown the potential for organic synthesis by natural clay minerals with transition-metal ions in exchange sites. Fewer studies have dealt with the effects of transition-metal ions in lattice sites. Wheeler and Thomas[6] provided evidence that Cu(II) cations in lattice sites in synthesized hectorite have a marked effect on the photochemistry of adsorbed [4-(1-pyrenyl)butyl]-trimethylammonium cation. Ni-substituted synthetic mica-montmorillonite clays have also been shown to be

(1) Coyne, L. M. In *Spectroscopic Characterization of Minerals and their Surfaces*, Coyne, L. M., McKeever, S. W. S., Blake, D. F., Eds.; ACS Symposium Series 415; American Chemical Society: Washington, D.C., 1990; Chapter 1.

(2) McCormack, G. R. *Clays Clay Miner.* **1978**, *26*, 93.

(3) Gerald, P.; Herbillon, A. J. *Clays Clay Miner.* **1983**, *31*, 143.

(4) Foord, E. E.; Starkey, H. C.; Taggart, J. E.; Shawe, D. R. *Clays Clay Miner.* **1987**, *35*, 139.

(5) Laszlo, P.; Mathy, A. *Helv. Chim. Acta* **1987**, *70*, 577.

(6) Wheeler, J.; Thomas, J. K. *Langmuir* **1988**, *4*, 543.

0897-4756/91/2803-1073$02.50/0

active hydroisomerization catalysts.[7-9]

Studies of transition-metal ions in lattice sites of smectite clays can be best studied by preparation of synthetic clays with specifically incorporated transition-metal ions. For example, for the smectite stevensonite, transition-metal cations may be readily incorporated into lattice sites in amounts ranging up to 50% octahedral occupancy.[10] When transition-metal cations can be substituted to such high concentrations, there should be a significant proportion of them accessible at edge lattice sites to interact with various Lewis base absorbate molecules and accomplish a variety of Lewis acid catalyzed reactions. Also the two-dimensional nature of smectite clays can have salutary effects on the kinetics of reactions occuring at their surfaces.[11]

The aim of the present work is to evaluate the incorporation of cupric ion into lattice sites of fluorohectorite and to study whether edge lattice sites with incorporated transition-metal ions such as cupric ion can interact to adsorb Lewis bases. This is a prelude to the possible utility of such systems for tailored catalytic reactions. The use of cupric ion as a probe is particularly advantageous in that its electron spin resonance spectrum is well studied and can be used to study the environment and local molecular interactions of the cupric ion with adsorbates. In addition pulsed electron spin resonance in the form of electron spin echo modulation spectroscopy can be used to determine the specific coordination numbers and information about the geometry of absorbate molecules interacting with the cupric ion.

Experimental Section

Copper(II)-substituted fluorohectorite (Cu-F-hect) was prepared by a method similar to that of Granquist and Pollock[12] and Wheeler and Thomas.[6] To prepare Cu-F-hect with 0.2% Cu, a wet gel was prepared with a composition corresponding to the chemical formula

$$Na_{0.5}(Mg_{2.49}Cu_{0.01}Li_{0.5})Si_4O_{10}F_2$$

The synthesis was as follows: Tetraethoxysilane (41.66 g, Baker, 99.6%) was added to 100 mL of ethanol and stirred at about 60 °C for 3 h. To this solution was added 21.31 g of $MgCl_2 \cdot 6H_2O$ (Baker, 99.7%) and 0.085 g of $CuCl_2 \cdot 2H_2O$ (Baker, 99.8%) dissolved in 200 mL of deionized water. This ethanol/water solution was stirred for at least 4 h, and then NaOH solution was added dropwise over a few minutes until a final pH of 9.5 was reached. After the solution was stirred for 12 h, the Mg/Si precipitate was filtered and washed. The solids were resuspended in deionized water, and 0.648 g of LiF (Fisher, AR) and about 3 g of NaF added. This suspension was stirred for about 12 h and then refluxed for 7 days. X-ray powder diffraction patterns of the suspension removed periodically from the reaction vessel indicated that crystallization of Cu-F-hect was essentially complete after 4 days of reflux.

The synthesized Cu-F-hect was treated with an ethylenediaminetetraacetic acid (EDTA)/sodium acetate pH = 5.5 buffer in order to remove possible exchangeable Cu(II) or surface-bound Cu(II) not part of the clay lattice. This was done by stirring each 1 g of smectite with 100 mL of the 10 mM EDTA buffer solution for 24 h and then repeating the treatment. The smectite suspension was filtered and then dialyzed to remove excess cations. At the end of 1 week of dialysis the suspension formed a stable transparent sol. After this sol stood for 1 week in a beaker, no particulate material had collected at the bottom of the beaker, indicating that the suspension consisted of pure smectite. A separate sample was Mg(II)-exchanged by stirring the smectite three times with 1 M $MgCl_2$ solution. The Mg(II)-exchanged Cu-F-hect was filtered, washed, and dialyzed to remove excess cations.

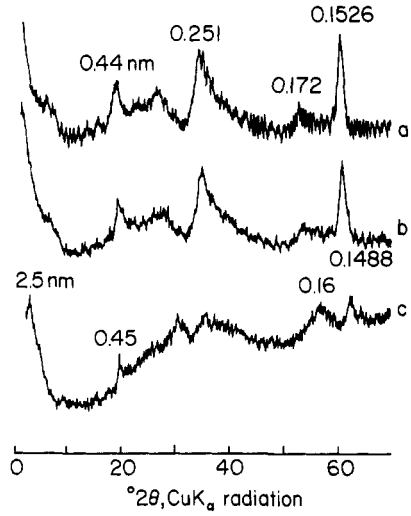

Figure 1. X-ray powder patterns of (a) commercial Laponite RD, (b) synthetic Cu-F-hect containing 0.2% Cu, and (c) synthetic totally Cu-substituted hectorite.

A Cu-F-hect sample was also synthesized in a similar manner from a gel with the composition

$$Na_{0.5}(Mg_{2.25}Cu_{0.25}Li_{0.5})Si_4O_{10}F_2$$

This composition corresponds to a Cu content of about 4%. Fluorohectorite phases of poor crystallinity were produced for Cu:Mg ratios greater than unity. To synthesize a smectite phase in which all the Mg(II) was replaced by Cu(II), a different method of synthesis was employed. A reactive dry gel was synthesized by the method of Hamilton and Henderson.[13] A Si/Cu precipitate was produced in a similar manner to that described above for the fluorohectorite. Nitrate metal salts were used instead of chlorides and fluorides, and in the final step the gel was first dried in an oven at 100 °C and then heated overnight in a furnace at 400 °C. This dry gel (12 g) was reacted with 180 ml of 0.1 M NaOH solution in a 1-L Parr bomb for 44 h.

X-ray powder diffraction (XRD) patterns of the synthetic Cu(II)-substituted fluorohectorites were recorded on a Philips PW1840 diffractometer and good agreement was obtained with the *d* spacings of the *hk* reflections of natural hectorite.[14]

Electron spin resonance (ESR) spectra were recorded at 77 K on a modified Varian E-4 ESR spectrometer. Electron spin echo modulation (ESEM) data were recorded at 4 K on a home-built spectrometer described previously.[15] Three-pulse stimulated echoes were recorded with a $\pi/2-\tau-\pi/2-T-\pi/2$ pulse sequence, and the echo was detected as a function of T, the time between the second and the third pulses. The time between the first and second pulse, τ, was chosen to maximize modulation from ^7Li or ^2H. Two-pulse echoes were recorded to observe ^7Li modulation in the absence of D_2O. Simulations were made in terms of N equivalent nuclei at a distance R and isotropic hyperfine coupling A using a spherical approximation.[16]

Activation of samples and exposure to the various adsorbates were carried out in a glass reactor to which was attached a Suprasil quartz ESR so that ESR spectra could be recorded without exposing the sample to the atmosphere. The reactor could be attached to a vacuum line. The adsorbates used were as follows: pyridine, C_5D_5N, 99 atom % D, Aldrich; benzene, C_6D_6, 99.96 atom

(7) Swift, H. E.; Black, E. R. *Ind. Eng. Chem. Prod. Res. Dev.* **1974**, *13*, 106.
(8) van Santen, R. A. *Recl. Trav. Chim. Pays-Bas* **1982**, *101*, 157.
(9) Gaff, J.; van Santen, R.; Knoester, R.; Wingerden, B. *J. Chem. Soc., Chem. Commun.* **1982**, 655.
(10) Mosser, C.; Mestdagh, M.; Decarreau, A.; Herbillon, A. J. *Clays Clay Miner.* **1990**, *25*, 271.
(11) Laszlo, P. *Science* **1987**, *235*, 1473.
(12) Granquist, W. T.; Pollack, S. S. *Am. Miner.* **1967**, *52*, 212.
(13) Hamilton, D. L.; Henderson, C. M. B. *Miner. Mag.* **1968**, *36*, 832.
(14) Brown, G.; Brindley, G. W. In *Crystal Structures of Clay Minerals and their X-Ray Identification*; Brindley, G. W., Brown, G., Eds.; Mineralogical Society: London, 1980; Chapter 5.
(15) Narayana, P. A.; Kevan, L. *Magn. Reson. Rev.* **1983**, *1*, 234.
(16) Kevan, L.; Bowman, M. K.; Narayana, P. A.; Boeckman, R. K.; Yudanov, V. F.; Tsvetkov, Yu. D. *J. Chem. Phys.* **1975**, *63*, 409.

Table I. ESR Parameters of Cu(II)-Montmorillontie and Cu(II)-Substituted Fluorohectorites

sample	T, K	$g_\parallel$	A^a	$g_\perp$	A	ref
MgCu-mont,	77	2.41	142	2.09		21
$d(001) > 2.01$ nm	300	$g_{iso} = 2.18$				
MgCu-mont,	77	2.35	178	2.07		21
$d(001) = 1.2$–1.7	300	2.35	175	2.07		
MgCu-mont,	77	2.42	117	2.09		21
$d(001) = 1.0$ nm	300	2.42	117	2.09		
Cu-mont, $d(001) = 1.25$	77	2.33	1.75	2.08		21
	300	2.34	165	2.08		
Cu-mont (Wy),	77	2.34	175	2.09		22
$d(001) = 1.25$ nm						
Cu(II)-sap,	77	2.35	180	2.08		22
$d(001) = 1.25$ nm	300	2.35	145	2.08		
MgCu-verm	300	2.40	123	2.09		36
gel	77	2.33	163	2.07	25	*b*
Cu-F-hect,	77	2.40	118	2.06		*b*
$d(001) = 1.25$ nm		2.26	50	2.08		

[a] Units of 10^{-4} cm^{-1}. [b] This work.

% D, Cambridge Isotope Laboratories (CIL); D_2O, 98 atom % D, Aldrich; ND_3, 99.5 atom % D, CIL; $^{15}NH_3$, 99.8 atom % ^{15}N, Aldrich.

Fourier transform infrared (FTIR) spectra were recorded on a Nicolet Model 740 FTIR spectrometer. Samples were prepared as pressed wafers of 10-mm diameter with the minimum amount of sample to optimize optical transparency.

Results

Characterization of Cu(II)-Substituted Fluorohectorite (Cu-F-hect). (i) X-ray Diffraction. The XRD pattern of the Cu-F-hect (Figure 1b) is similar to that of natural hectorite[14] and commercially available Laponite RD (Figure 1a) and shows no evidence of impurity phases.

To provide further evidence that Cu(II) is capable of substituting for Mg(II), an attempt was made to synthesize a totally Cu(II)-substituted hectorite sample (i.e., no Mg(II) included in the synthesis mixture) made from a gel with the composition

$$Na_{0.5}(Cu_{2.5}Li_{0.5})Si_4O_{10}(OH)_2$$

The XRD pattern of the product is shown in Figure 1c. It is evident that a number of relatively intense reflections are present at angles below 2θ of 5°. These reflections and *hk* reflections with $d = 0.45$, 0.25, 0.161, and 0.1488 nm indicate that a smectite phase formed. It would appear therefore that Cu(II) is indeed capable of substituting Mg(II). No attempt was made to optimize the yield of this synthesis since the intention in the present work was simply to demonstrate that smectite phases can be formed from compositions with no Mg(II).

(ii) Electron Spin Resonance. Quantitative ESR measurements on the "as-synthesized" Cu-F-hect containing 0.2% Cu after EDTA treatment and on a Mg(II)-exchanged sample, indicated that EDTA treatment and Mg(II) exchange result in the removal of less than 20% of the Cu(II) originally present. This implies that most of the Cu(II) indeed resides within the fluorohectorite lattice since EDTA complexes Cu(II) very strongly and is expected to remove it easily from surface sites. In contrast, treatment of Cu(II)-exchanged fluorohectorite with the EDTA buffer solution successfully removed more than 90% of the exchangeable Cu(II). All subsequent experiments have been carried out on EDTA-treated samples of Cu-F-hect containing 0.2% Cu.

The ESR spectrum of both the starting gel and the Cu-F-hect product with 0.2% Cu are shown in Figure 2 and the parameters are given in Table I. Both starting material and product gave ESR signals characteristic of Cu(II) in sites of axial symmetry. There are obvious differences between these two spectra which testify to a change in the environment of the Cu(II) after reaction.

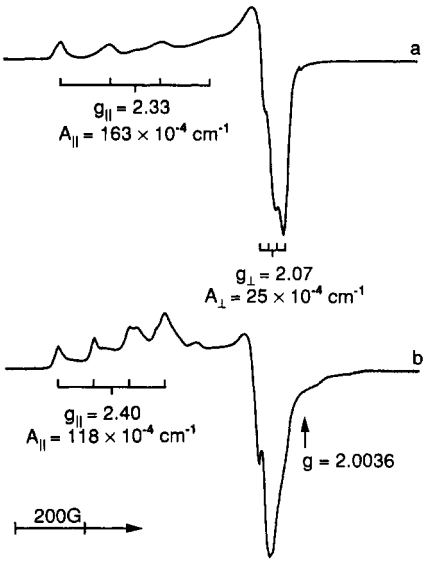

Figure 2. ESR spectra at 77 K of (a) gel for the synthesis of Cu-F-hect containing 0.2% Cu, and (b) Cu-F-hect containing 0.2% Cu.

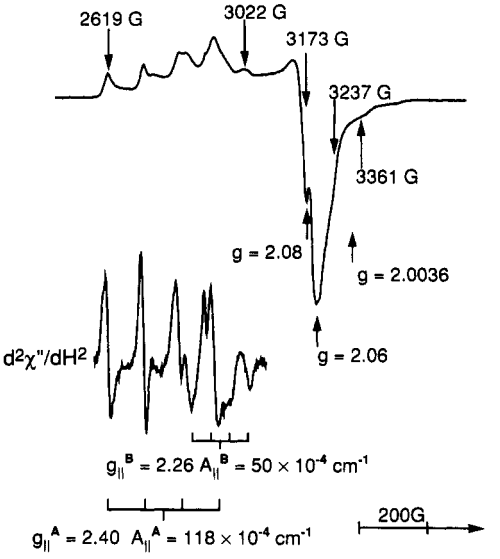

Figure 3. ESR spectra at 77 K of Cu-F-hect containing 0.2% Cu showing the second derivative of the $g_\parallel$ region.

The ESR spectrum of the synthetic fluorohectorite is shown in Figure 3. At least two signals are evident, one with $g_\parallel = 2.40$ and $A_\parallel = 118 \times 10^{-4}$ cm^{-1} referred to as species A and another with $g_\parallel = 2.26$ and $A_\parallel = 50 \times 10^{-4}$ cm^{-1} referred to as species B. The two separate species are even more obvious in the second derivative spectrum shown in Figure 3 and labeled as $d^2\chi''/dH^2$. In the perpendicular region of the spectrum of Figure 3 at least two $g_\perp$ signals are evident. These two signals will be assigned somewhat arbitrarily for the present as $g_\perp^A = 2.06$ and $g_\perp^B = 2.08$. The order of this assignment has little bearing on the subsequent discussion, and therefore no justification for the present assignment will be given herein but will be provided in a subsequent publication. It should be noted that poorly resolved resonances are also discernible at 3272 and 3361 G. The ESR spectrum of a water-soaked sample of Cu-F-hect gave an anisotropic signal at room temperature.

(iii) Electron Spin Echo Modulation. Two-pulse ESEM data were recorded at the field positions marked

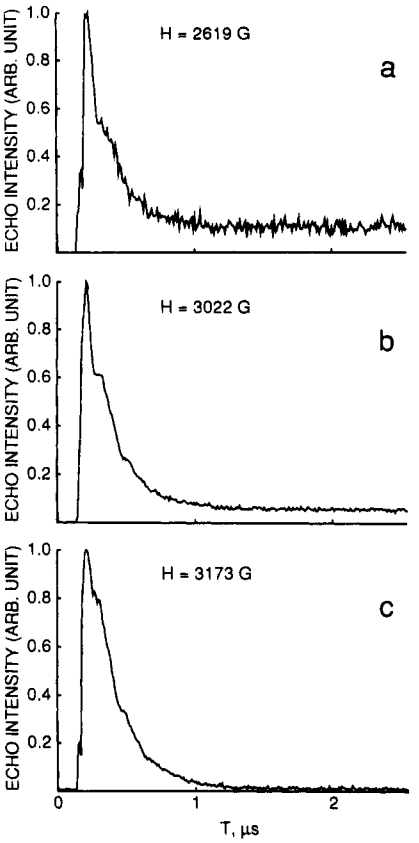

Figure 4. Two-pulse ESEM signals at 4 K and at various fields of Cu-F-hect containing 0.2% Cu equilibrated at 100% RH at (a) 2619, (b) 3022, and (c) 3173 G.

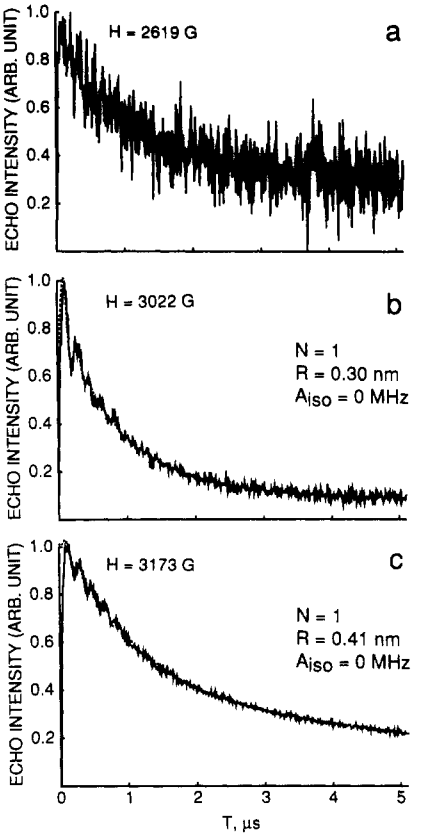

Figure 5. Three-pulse ESEM signals at 4 K and at various fields of Cu-F-hect containing 0.2% Cu equilibrated at 100% RH at (a) 2619, (b) 3022, and (c) 3173 G.

by the arrows (2619, 3022, 3173 G) in Figure 3, and the results are given in Figure 4. In Figure 3 the line at 2619 G corresponds fairly certainly to only species A, the line at 3022 G probably to species B only (see second-derivative spectra in Figure 3b), and the line at 3173 G probably to both species. The two-pulse ESEM relative modulation depths seem to be greatest at 3022 G (Figure 4b), next greatest at 3173 G (Figure 4c), and smallest at 2619 G (Figure 4a). This indicates that the Li(I) cations are closer to species B than to species A.

Three-pulse ESEM data are presented in Figure 5. The echo obtained for the ESR line at 2619 G was very weak. Even so, no modulation could be discerned (Figure 5a). For the line at 3022 G, a reasonably strong echo was observed (Figure 5b) and the ESEM was simulated with $N = 1$ and $R = 0.30$ nm, while the line at 3173 G gave the ESEM signal of Figure 5c which was simulated with $N = 1$ and $R = 0.41$ nm.

Interaction of Cu(II) in Cu(II)-Substituted Fluorohectorite with Adsorbates. (i) Electron Spin Resonance. *Ammonia*: Ammonia is a good Lewis base and should therefore form strong complexes with Lewis acid sites on the clay mineral surfaces. Presumably these will be Cu(II) sites on the clay mineral edges since Cu(II) not on the crystal edges will be inaccessible to ammonia.

The fluorohectorite surface was first activated to remove adsorbed water and hydroxyl groups. This was done by heating a 40-mg sample at 5 mTorr for 2 h followed by heating at the same temperature in flowing oxygen to reoxidize any Cu(I) formed during vacuum dehydration. The sample was then exposed to 200–500 Torr of ND_3 for about 12 h. Following adsorption, excess ammonia was removed by evacuation to 5 mTorr. The results of activation at various temperatures are shown in Figure 6. An increase in activation temperature results in the progressive increase in the intensity of a signal at about $g = 1.98$ and also an increase in the resolution of ^{14}N hyperfine splitting at fields higher than 3207 G. This indicates that ammonia is directly coordinating some Cu(II) sites in the fluorohectorite lattice. On the basis of these results, the adsorption of other molecules was studied after activation

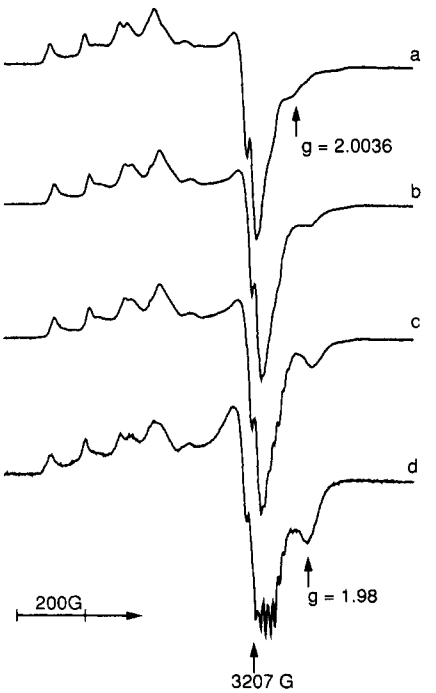

Figure 6. ESR spectra at 77 K of Cu-F-hect containing 0.2% Cu and adsorbed ND_3 after activation at (a) 100, (b) 200, (c) 300, and (d) 400 °C.

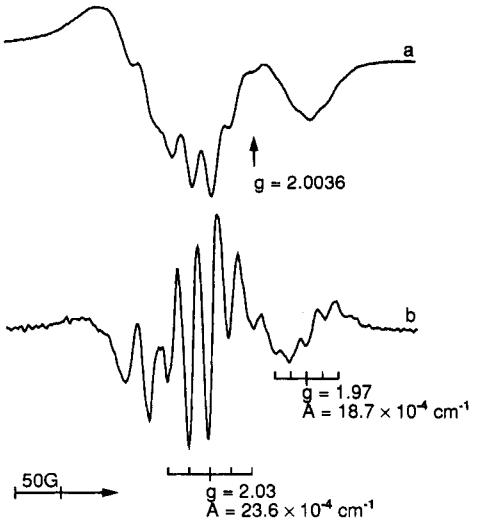

Figure 7. ESR spectra at 77 K in the $g_\perp$ region of Cu-F-hect containing 0.2% Cu after activation at 400 °C and adsorption of $^{15}NH_3$ (a) first-derivative spectrum and (b) second-derivative spectrum.

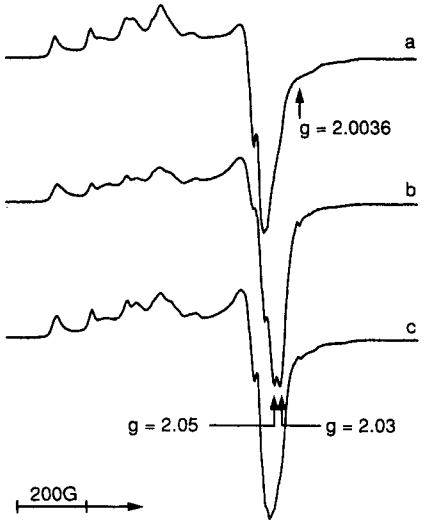

Figure 8. ESR spectra at 77 K of Cu-F-hect containing 0.2% Cu at (a) ambient relative humidity, (b) activated at 400 °C, and (c) sample from (b) equilibrated at 100% relative humidity.

at 400 °C. No nitrogen superhyperfine splitting of any of the ESR signals from species A or B was observed. No electron spin echo could be detected in any of the samples containing adsorbed ammonia.

A sample of Cu-F-hect that had been activated at 400 °C was exposed to about 200 Torr of $^{15}NH_3$ for 12 h and then evacuated at 2 mTorr. The ESR spectrum of this sample in the $g_\perp$ region is shown in Figure 7a, and the second derivative of this region is shown in Figure 7b. The first two lines in the second-derivative spectrum are probably $g_\perp{}^A$ and $g_\perp{}^B$ because their separation is slightly larger than lines at higher fields. This assignment is discussed in greater detail later. The next five lines have a regular separation of 23.6 G, and the splittings of the "overshoot" transition at about $g = 1.97$ are measurably smaller at about 19 G.

Water: The effect of activation at 400 °C and rehydration with D_2O is shown in Figure 8. The fluorohectorite at ambient relative humidity (RH; Figure 8a) gives species A and B with $g_\parallel$ components that are clearly visible as mentioned above. In the $g_\perp$ region two signals are discernible which are assigned to $g_\perp{}^B = 2.08$ and $g_\perp{}^A = 2.06$ or vice versa. At still higher fields two shoulders

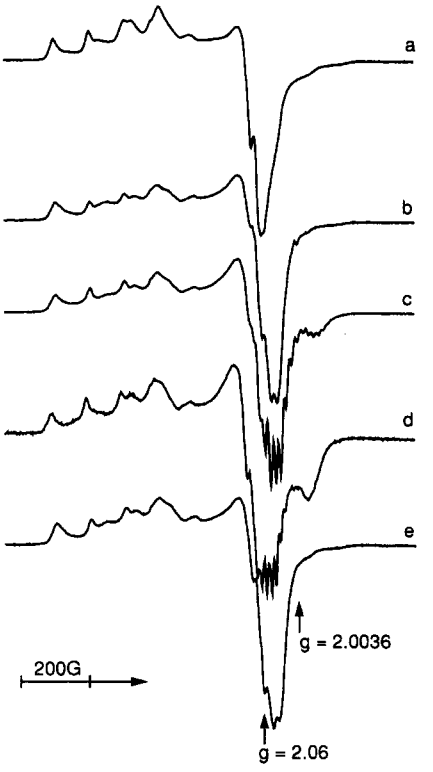

Figure 9. ESR spectra at 77 K of samples of Cu-F-hect containing 0.2% Cu (a) sample at ambient relative humidity, (b) sample activated at 400 °C, (c) sample from (b) after adsorption of pyridine, (d) sample from (b) after adsorption of ammonia, and (e) sample from (b) after adsorption of benzene.

are evident at 3237 and 3361 G, and when water is removed by activation at 400 °C (Figure 8b), two further signals at $g = 2.05$ and $g = 2.03$ take the place of the shoulder at 3237 G. Adsorption of D_2O by the activated sample results in a spectrum (Figure 8c) that is very similar to the fluorohectorite before activation (Figure 8a). The signals at $g = 2.03$ and $g = 2.05$ do not appear to be Cu ($I = {}^3/_2$) hyperfine and neither do they appear to be related to Cu(II) species A and B. They will be termed species C sites. These results suggest that the removal of water and OH groups from the fluorohectorite surfaces generate Cu(II) in environments (species C) different from those of species A and B so that separate resonances are resolved. It is suggested that the Cu(II) species C contributing to these new resonances are due to Cu(II) at edge lattice sites, since Cu(II) in the interior of an octahedral sheet in the fluorohectorite crystallites are not expected to be so affected by the removal of water.

Pyridine and benzene: Since it appears that edge lattice Cu(II) sites are detected in the Cu(II) ESR spectrum of the fluorohectorite samples, the interaction of Cu(II) with other adsorbate molecules was examined. These other adsorbates include the π-electron donor base, benzene, and the nitrogen lone-pair base, pyridine. The results of adsorption of these Lewis bases with fluorohectorite samples activated at 400 °C are collected in Figure 9. For clarity the spectra of unactivated and activated fluorohectorite are reproduced in this figure. Regardless of the adsorbate, it appears that the g components of species A and B remain invariant. For adsorbates with nitrogen donor ligands, N hyperfine is observed at fields higher than the species C $g = 2.03$ signal replacing the two resonances of the edge lattice Cu(II) species. Moreover, it is evident that in the case of pyridine (Figure 9c), the species C resonances which exhibit nitrogen superhyperfine splitting are shifted to higher g values compared to the sample containing

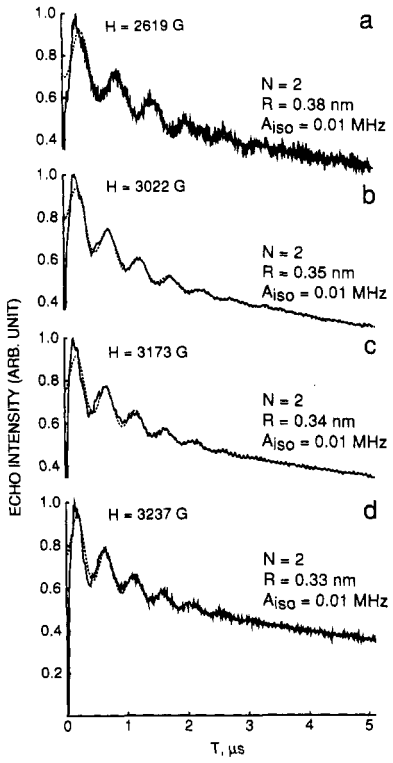

Figure 10. Three-pulse ESEM data at 4 K and at various fields of Cu-F-hect containing 0.2% Cu activated at 400 °C and then equilibrated at 100% RH D_2O at (a) 2619, (b) 3022, (c) 3173, and (e) 3237 G.

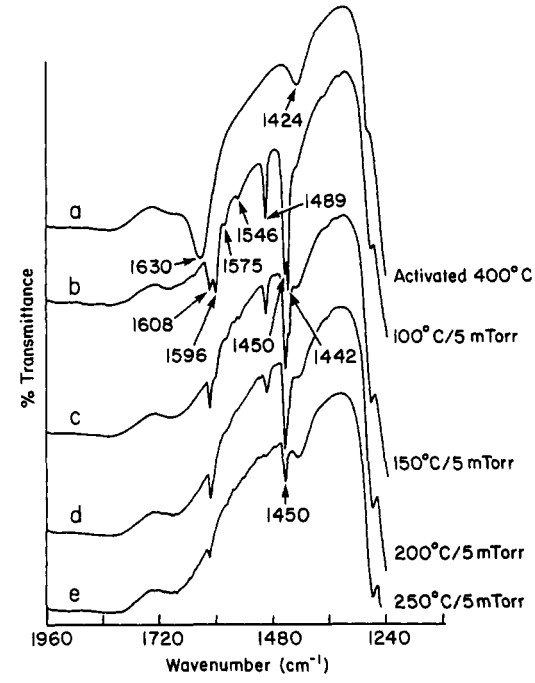

Figure 11. FTIR of Cu-F-hect containing 4% Cu (a) activated at 400 °C, (b) sample from (a) after adsorption of pyridine and evacuation at 100 °C, (c) sample from (b) evacuated at 150 °C, (d) sample from (c) evacuated at 200 °C, and (e) sample from (d) evacuated at 250 °C.

adsorbed ammonia (Figure 9d). The adsorption of benzene does not appear to have any effect on the Cu(II) ESR signals of the edge lattice Cu(II) sites. This is not unexpected since benzene is expected to coordinate with a configuration parallel to the fluorohectorite edge surface. This type of coordination may be sterically hindered by the nature of the edge surface.

(ii) Electron Spin Echo Modulation. *Water*: To obtain information on the number of adsorbate molecules coordinated to each Cu(II) site, ESEM has been used. The adsorption of water was investigated on samples activated at both 100 and 400 °C and then equilibrated in a 100% RH D_2O atmosphere. ESEM data that were recorded at 2619, 3022, and 3173 G (Figure 3) of samples that were activated at 400 °C and then equilibrated at 100% RH D_2O are shown in Figure 10. These fields correspond to Cu(II) species A and B. ESEM signals are obtained that are best simulated by $N = 2$ and $R = 0.34$–0.38 nm. This distance is too long to involve *direct* coordination of water molecules to Cu(II) species A and B as expected since these are not at edge lattice sites. In addition to the three fields indicated in Figure 3 (2619, 3022, and 3173 G), ESEM data were recorded at 3237 G in an attempt to sample species C. Attempts made to acquire ESEM data at higher fields than 3237 G were not fruitful. For ESEM data recorded at 3237 G, however, the best simulations are obtained for $N = 2$ and $R = 0.33$ nm. This distance is somewhat shorter than that obtained from ESEM data taken at lower fields where species A and B dominate and correspond to the outer limits of the distance expected for direct coordination. Because the field at 3237 G represents absorption from several Cu(II) species, including the putative edge lattice Cu(II) sites, the shorter Cu(II)–D distance at this field suggests that the Cu(II) C species contributing to the shoulder at 3237 G are directly coordinated to water molecules as expected for an edge lattice site. Similar results to these were obtained for samples that were activated at 100 °C and then equilibrated in 100% RH in D_2O.

Ammonia, pyridine, and benzene: Attempts to obtain electron spin echoes for samples with these adsorbates were unsuccessful. Judging from the reduction in echo intensity consistently observed for decreased hydration several different kinds of paramagnetic transition-metal ions in both smectities and zeolites, the intensity of the electron spin echo may be diminished by aggregation of exchangeable cations on dehydration.

Characterization of Acid Sites on Cu(II)-Substituted Fluorohectorite. (i) FTIR Spectroscopy of Adsorbed Pyridine. To characterize the acidity of Cu-F-hect, a sample was prepared with Cu content of about 4% Cu and this was EDTA treated. When pyridine is adsorbed on Bronsted acid sites, the base is protonated and the characteristic bands of the pyridinium ion are observed at 1490, 1540, 1620, and 1640 cm^{-1}. If pyridine is coordinated to a Lewis acid site the characteristic bands of adsorbed pyridine are observed at 1450, 1490, 1580, and 1600–1630 cm^{-1}.[17,18]

A pressed wafer of Cu(II)-substituted fluorohectorite was activated at 400 °C and then exposed to pyridine vapor for 12 h. The sample was then degassed and subsequently heated at various temperatures under a dynamic vacuum of 5 mTorr for 1 h. The FTIR spectrum of the activated sample shows a broad band near 3400 cm^{-1} corresponding to the stretching vibration of adsorbed water molecules. The part of this spectrum shown in Figure 11a possesses a band at 1630 cm^{-1} which corresponds to the bending vibrations of adsorbed water. Thus, even under the present activation conditions some adsorbed water appears to be present in the clay. This has been previously observed and attributed to water trapped within pseudohexagonal (ditrigonal) cavities when the clay interlayers collapse.[19] The origin of the band at 1424 cm^{-1} is not

(17) Kiviat, F. E.; Petrakis, L. *J. Phys. Chem.* **1973**, *77*, 1232.
(18) Parry, E. P. *J. Catal.* **1963**, *2*, 371.

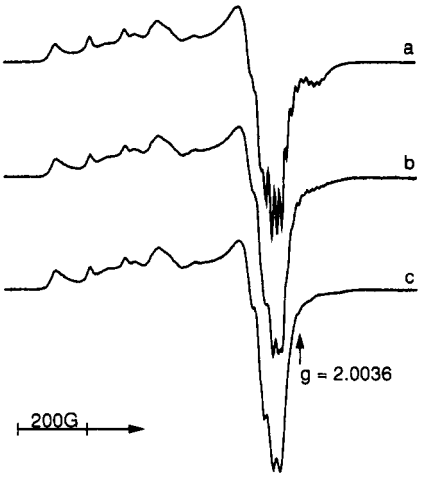

Figure 12. ESR spectra at 77 K at Cu-F-hect containing 0.2% Cu activated at 400 °C and adsorbed with NH_3 (a) evacuated at room temperature, (b) sample from (a) evacuated at 100 °C, and (c) sample from (b) evacuated at 200 °C.

certain but could be due to an N–H stretching vibration associated with the fact that the sample was treated with EDTA to remove surface Cu(II).

Heating the Cu(II)–fluorohectorite under vacuum for 1 h generates a series of bands in the 1360–1720-cm^{-1} region of the spectrum (Figure 11b). These bands are due to pyridine adsorbed on Lewis acid sites present on the fluorohectorite surfaces. Increasing temperature causes the bands at 1596 and 1442 cm^{-1} to decrease in intensity relative to the bands at 1608 and 1450 cm^{-1} (Figure 11c,d) until at 250 °C only one type of bound pyridine is observed. This indicates that there are two types of Lewis acid sites of differing acid strength. The weak band at 1546 cm^{-1} in Figure 10b is due to a small proportion of Bronsted acid sites.

The FTIR spectrum of a similarly treated sample of fluorohectorite containing no Cu(II) was also recorded after evacuation at 150 °C. For this sample, bands due to pyridine bound to a Lewis acid site were observed at 1442, 1492, and 1596 cm^{-1}. Therefore the bands at these positions in the Cu-F-hect samples are due to pyridine bound to Lewis acid sites intrinsic to the fluorohectorite and are unrelated to Cu(II) sites.

(ii) ESR of Adsorbed Pyridine. To see if the results of the FTIR study have some correspondence with ESR, a sample of Cu-F-hect was treated similarly as the samples examined by FTIR. Evacuation at 100 °C (Figure 12b) results in the removal of the "overshoot" signal at $g = 1.98$, though the ^{14}N splitting of pyridine (C_6D_5N) directly bound to Cu(II) can still be observed. Only very weak ^{14}N hyperfine structure can be observed after heating to 200 °C (Figure 12c). This lends support to the assignment of the higher frequency band of pyridine bound to Lewis acid sites to pyridine bound to Cu(II) edge lattice sites.

Discussion

Location of Cu(II). Initial evidence for the substitution of Cu(II) into the lattice of fluorohectorite comes from the fact that EDTA treatment removes only a small amount of Cu(II) from the freshly synthesized fluorohectorite when Cu(II) was included in the synthesis mixture. In contrast, most of the Cu(II) can be removed from synthetic fluorohectorite in which no Cu(II) was included in the synthesis mixture but which was completely Cu(II)-exchanged. This suggests that the bulk of the Cu(II) in Cu-F-hect is more strongly bound than most of the Cu(II) in Cu(II)-exchanged fluorohectorite with the implication being that in the former the Cu(II) is incorporated into the fluorohectorite lattice.

Considering the similarity of the ionic radius and charge of Cu(II) and Mg(II), the isomorphous substitution of Mg(II) by Cu(II) in the octahedral sheet can be anticipated. The ability to synthesize a smectitic phase from a synthesis mixture in which there is no Mg(II) is a good indication that Cu(II) is able to assume 6-fold coordination and form an octahedral sheet similar to that of Mg(II). It is considered unlikely that Cu(II) will substitute for Si(IV) in the tetrahedral sheet. Partition coefficients have been determined between trioctahedral smectites and transition metal ion aqueous solutions and it was found that Ni(II), Co(II), Zn(II), and Cu(II) are all strongly stabilized in the octahedral layer of smectites compared with Mg(II).[20] The highest partition coefficient was found for Cu(II). Recently, Mosser et al.[10] provided X-ray absorption fine structure and ESR evidence for the substitution of Cu(II) for Mg(II) in the octahedral sheet for Cu/(Cu + Mg) ratios up to 0.5 in the lattice of stevensonite, a smectite related to fluorohectorite. These are therefore supporting reasons to believe that some Cu(II) can substitute for Mg(II) in the octahedral sheet of the fluorohectorite structure.

The $A_\parallel$ values for both species A and B in the ESR spectrum of Cu-F-hect containing 0.2% Cu(II) are different from those obtained for Cu(II)-exchanged hydrated montmorillonite which gives $A_\parallel = 142 \times 10^{-4}$ cm^{-1} in the wet state and 178×10^{-4} cm^{-1} at 100% RH.[21] However, the $A_\parallel$ value of species A in Cu-F-hect at ambient humidities is similar to the $A_\parallel$ value of 117×10^{-4} cm^{-1} in dehydrated Cu(II)-exchanged montmorillonite[21] where the Cu(II) is assigned to a hexagonal cavity in the basal oxygen surface of the interlayer space and by the value of about 110×10^{-4} cm^{-1} obtained for Cu(II) in Cu(II)-substituted stevensonite.[6] Stevensonite is a trioctahedral smectite similar by hectorite except that there are no Li(I) ions and the layer charge is created by vacancies in the octahedral sheet.

Another significant result is that the ESR spectrum of a water-soaked sample of the Cu-F-hect recorded at room temperature gave an anisotropic signal. In contrast, water-soaked smectite samples containing exchangeable Cu(II) usually exhibit isotropic signals due to rapid tumbling of the hydrated Cu(II) species.[10,21-24] The observation of anisotropic signals for water-soaked Cu-F-hect indicates that the Cu(II) cations in hydrated Cu-F-hect are not free to tumble. This is consistent with the siting of Cu(II) in a fluorohectorite lattice.

At least three types of Cu(II) are expected a priori in Cu-F-hect. Within the clay crystallites Cu(II) is expected to populate, with roughly equal probability, sites neighboring an octahedron containing Li(I) and sites not neighboring Li(I) containing octahedra. The ionic radii of Mg(II), Cu(II), and Li(I) are 0.72, 0.73, and 0.76 nm respectively. Hazen and Wones[25] have shown that in trioctahedral micas the size of the octahedral sheet increases as the size of the octahedral cation increases. Therefore, it is expected that a Li(I)-containing octahedron is larger than a Mg(II)- or Cu(II)-containing octahedron

(19) Suquet, H.; Prost, R.; Pezerat, H. *Clay Miner.* **1982**, *7*, 231.

(20) Decarreau, A. *Cosmochim. Acta* **1985**, *49*, 1537.
(21) Brown, D. R.; Kevan, L. *J. Am. Chem. Soc.* **1988**, *110*, 2743.
(22) Clementz, D. M.; Pinnavaia, T. J.; Mortland, M. M. *J. Phys. Chem.* **1973**, *77*, 196.
(23) McBride, M. B.; Mortland, M. M. *Soil Sci. Soc. Am. Proc.* **1974**, *38*, 408.
(24) McBride, M. B. *Clay Clays Miner.* **1982**, *30*, 200.
(25) Hazen, R. M.; Wones, D. R. *Am. Miner.* **1972**, *57*, 103.

and that if an octahedron containing Cu(II) neighbors an octahedron containing Li(I), the Cu(II) octahedron is more distorted than a Cu(II)-containing octahedron with no neighboring Li(I)-containing octahedron. Thus, as a working hypothesis, species A and B will be considered to correspond to Cu(II)-containing octahedra with and without neighboring Li(I)-containing octahedra. This was verified by ESEM since the ESE signal of a Cu(II) site proximal to a Li(I) site should show modulations with the nuclear frequency of ^{7}Li. This is what is observed experimentally; the ESR line at 3022 G corresponding to species B gives the strongest Li modulation. Since the line at 2619 G corresponding only to species A gave very weak modulation and since the line at 3237 G is the sum of both species A and B, it is not surprising that at 3237 G the modulation depth is intermediate between that at 2619 and 3022 G and that the distance from the simulations at the 3237-G line is close to that at the 3022-G line. The distance of about 0.3 nm between Cu(II) and ^{7}Li(I) from the simulation of data recorded at the 3022-G line is in agreement with the expected Cu–Li distance for Cu(II) and Li(I) in neighboring octahedra in the fluorohectorite lattice. This is strong confirmation of the proposed model.

Three-pulse ESEM data recorded at the ESR lines corresponding to species a or B of samples that were activated at 100 or 400 °C and then equilibrated in 100% RH of D_2O could all be simulated with $N = 2$ and $R =$ 0.33–0.40 nm. These distances are too large to correspond to direct coordination of water molecules to these Cu(II) sites and therefore indicate that species A and B are not accessible to water. These results contrast with ESEM data recorded for exchangeable Cu(II) in hydrated montmorillonite which indicate 12 deuterons at a distance of 0.29 nm.[21] There is therefore a dramatic difference between the solvation of exchangeable Cu(II) in montmorillonite and Cu(II) species A and B in Cu-F-hect. On the basis of the preceding discussion, it is clear that species A and B correspond to Cu(II) sites within the octahedral sheet of the fluorohectorite lattice layers.

(b) Adsorbate Interactions. We now consider the adsorption of Lewis base molecules by synthetic Cu-F-hect. The results showing the effects of the desorption and readsorption of water on ESR spectra of Cu-F-hect (Figure 8) suggest that water is able to interact with certain Cu(II) sites on the Cu-F-hect surfaces. However, ESEM studies of Cu-F-hect samples activated at 100 and 400 °C and then allowed to adsorb D_2O do not show direct coordination of water molecules to species A and B Cu(II) sites. Of all the simulations, R is the shortest for the ESEM data taken at 3237 G corresponding at least in part to Cu(II) species C which is assigned to edge lattice sites. From this it is inferred that D_2O is directly coordinated to Cu(II) species C sites. The inability to provide more definitive evidence for the coordination of water molecules to some Cu(II) sites of the Cu-F-hect is a result of there being several overlapping signals in the $g_\perp$ region of the spectrum.

More satisfactory results are obtained using nitrogen-donor bases such as ammonia and pyridine for which direct coordination to some Cu(II) is established by the presence of a nitrogen superhyperfine interaction. Both ammonia and pyridine give a superhyperfine splitting at the g^c position on the high-field side of $g_\perp{}^A$ and $g_\perp{}^B$ as well as a so-called "overshoot" transition due to an intermediate turning point between $g_\parallel$ and $g_\perp$. Such overshoot transitions have been observed in copper phthalocyanine complexes,[26] copper in galactose oxidase,[27] and Cu(II)–ammine complexes in zeolites.[28,29] Since there is no ^{14}N superhyperfine splitting of $g_\perp{}^A$ and $g_\perp{}^B$ or of any of the $g_\parallel$ transitions, this indicates that ammonia and pyridine cannot coordinate to Cu(II) species A and B. It would seem, therefore, that the poorly resolved signals near 3237 G (species C) arise from Cu(II) sites which are part of the octahedral sheet of the Cu-F-hect and which are exposed to, and can interact with, adsorbate molecules. The appearance of the "overshoot" transition after adsorption of ammonia or pyridine indicates that Cu(II)^C sites have axial symmetry after adsorption. This is consistent with saturation of the coordination around the edge Cu(II)^C sites. The adsorption of $^{15}NH_3$ apparently results in the splitting of the "overshoot" line into probably four lines. Because ^{15}N has $I = {}^1/_2$, this implies that the Cu(II)^C species responsible for this transition is directly coordinated to three NH_3 molecules. For the sample containing adsorbed pyridine ($C_5{}^{14}ND_5$), the "overshoot" transition is split into five or six lines, indicating coordination of each Cu(II)^C site to two or three pyridine molecules. These coordination numbers seem consistent with additional coordination to three or four lattice oxygens to retain octahedral coordination at an edge lattice site. Washing with water does not indicate that Cu(II) is being extracted from the lattice by these adsorbates.

A number of studies have shown that benzene interacts with Cu(II)-exchanged montmorillonites and hectorites.[30-32] In these systems several different benzene radicals were reported to form upon adsorption. The type of radical formed is apparently dependent on the hydration state. When benzene is adsorbed on the surfaces of Cu-F-hect, no such benzene radicals are observed and the ESR spectrum of the activated Cu-F-hect sample exposed to benzene is identical to that of an activated sample (Figure 9), indicating that benzene cannot interact with interior lattice or edge lattice Cu(II) sites of the Cu-F-hect. Thus, there is a fundamental difference between the adsorbate interactions of exchangeable Cu(II) and substituted Cu(II). Since benzene is a π-donor Lewis base which coordinates to Lewis acids through the planar π-electron system, one reason that benzene may not complex Cu(II) at edge lattice sites of Cu-F-hect is that it is sterically hindered from approach to these sites. The Cu-F-hect surface appears to impose steric constraints on the type of molecules that can be coordinated which implies potential selectivity.

The present results demonstrate that certain sites on Cu-F-hect surfaces are able to adsorb certain Lewis base molecules. These Cu(II) sites have moderate Lewis acid strength as indicated by FTIR. Cu(II) at edge lattice sites are implicated in this adsorption process. These sites may be utilizable in reactions involving Lewis acid catalysis. Prior to this work, the ability of transition-metal ions in a smectite lattice, as opposed to exchangeable transition-metal ions, to coordinate adsorbate molecules has not been demonstrated to our knowledge. We have shown that the propensity of a smectite lattice for adsorption of certain molecules can be increased by the incorporation of transition-metal cations into lattice sites. This is of particular value for smectite clays because of the advantages of small particle size and therefore the large proportion of edge surface area to total surface area and because of the pos-

(26) Nieman, R.; Kivelson, D. *J. Phys. Chem.* **1973**, *77*, 1232.
(27) Bereman, R. D.; Kosman, D. J. *J. Am. Chem. Soc.* **1977**, *99*, 7322.
(28) Naccache, C.; Ben Taarit, Y. B. *Chem. Phys. Lett.* **1971**, *11*, 11.
(29) Flentge, D. R.; Lunsford, J. H.; Jacobs, P. A.; Uytterhoeven, J. B. *J. Phys. Chem.* **1975**, *79*, 354.
(30) Donor, H. E.; Mortland, M. M. *Science* **1969**, *166*, 1406.
(31) Pinnavala, T. J.; Hall, P. L.; Cady, S.; Mortland, M. M. *J. Phys. Chem.* **1974**, *78*, 994.
(32) Eastman, M. P.; Patterson, D. E.; Pannell, K. H. *Clays Clay Miner.* **1984**, *32*, 327.

sible reduction in reaction dimensionality.[11] Moreover, the ability to replace the more common octahedral lattice cations, Al(III) and Mg(II), with transition-metal cations suggests that new active sites can be generated.

Further tuning of the surface properties of such systems is possible by the implementation of other approaches. Certain transition-metal cations may be substituted for Si(IV) in the tetrahedral sheet in addition to or instead of substitutions in the octahedral sheet. Coordinatively unsaturated sites in the tetrahedral sheet should have even stronger Lewis acid strength than coordinatively unsaturated sites in the octahedral sheet because the lower the coordination number the greater should be the Lewis acidity. An example is the mineral sauconite[33] with the ideal chemical formula $(Zn_6)Si_{8-x}Zn_xO_{10}(OH)_2$. It may also be possible to gain some synthetic control over the particle size and hence the proportion of edge surface sites available. Finally, the exchange capacity of such transition-metal-substituted smectite clays can be exploited for more traditional modification of surface properties.

Conclusions

Fluorohectorite clay was synthesized in which Cu(II) is substituted for Mg(II) in the octahedral sheet. These results provide reasonably definitive evidence for this substitution which has also been suggested for the related mineral stevensonite.[10,34] Copper(II) does not seem to preferentially occupy one type of site with respect to Li(I) substitution. We have also demonstrated that total substitution of Cu(II) for Mg(II) can be achieved.

A consequence of Cu(II) for Mg(II) substitution is that some of the Cu(II) exists at edge lattice sites of the fluorohectorite crystals. These are coordinatively unsaturated and are capable of binding Lewis base adsorbate molecules, apparently with some degree of selectivity. The substitution of one or a combination of transition-metal ions in different lattice sites may represent a means of tailoring smectite surface acidity for specific catalytic applications.

Acknowledgment. This work was supported by the Robert A. Welch Foundation, the Texas Advanced Research Program, and the National Science Foundation.

Registry No. NH_3, 7664-41-7; H_2O, 7732-18-5; C_6H_6, 71-43-2; Cu^{2+}, 15158-11-9; $Na_{0.5}(Mg_{2.49}Cu_{0.01}Li_{0.5})Si_4O_{10}F_2$, 136952-82-4; $Na_{0.5}(Mg_{2.25}Cu_{0.25}Li_{0.5})Si_4O_{10}F_2$, 136952-81-3; $Na_{0.5}(Cu_{2.5}Li_{0.5})Si_4O_{10}(OH)_2$, 136952-80-2; pyridine, 110-86-1; hectorite, 12173-47-6.

(33) Donor, H. E.; Mortland, M. M. *Science* **1981**, *166*, 1406.

(34) McBride, M. B. *Clays Clay Miner.* **1976**, *24*, 211.

Infrared Studies of CO Adsorption on Rhodium Hydrosols

M. R. Mucalo and R. P. Cooney*

Chemistry Department, University of Auckland, Private Bag, Auckland, New Zealand

Received May 24, 1991. Revised Manuscript Received August 26, 1991

Infrared spectra of CO adsorbed on poly(vinyl alcohol)-protected rhodium hydrosols exhibit two bands in the regions 2030–2040 and 1890–1900 cm^{-1}, which have been assigned respectively to CO adsorbed on linear and 2-fold-bridging rhodium metal surface sites. The band positions for adsorbed CO species on rhodium resemble those observed in infrared spectra of CO adsorbed on polycrystalline rhodium electrodes. When the pH was adjusted above the natural hydrosol pH of ca. 2.2, $\nu(CO)_{ads}$ was observed to decrease. This was attributed to the lower CO coverage resulting from hydroxyl adsorption and to surface oxide formation on the rhodium particles. Values of $d\nu/d\psi_0$ derived from $d\nu/d(pH)$ values for CO adsorbed on rhodium hydrosol particles (pH < ca. 2.2) were in the range 26–40 cm^{-1} V^{-1}. These were similar to values reported from in situ spectroelectrochemical studies of CO adsorbed on polycrystalline rhodium electrodes (40 cm^{-1} V^{-1}) and of CO adsorbed on single-crystal rhodium electrodes (35 cm^{-1} V^{-1}) in acidic media, thus indicating similarities between adsorption on electrode and colloid surfaces. X-ray photoelectron spectra of rhodium flocs prepared in the absence of poly(vinyl alcohol) revealed the presence of surface Rh_2O_3 and residual $RhCl_3$.

Introduction

Previous work has centered on characterizing CO adsorbed on platinum and palladium colloids in various dispersion media. For example, infrared spectra of CO adsorbed on colloidal platinum in CH_2Cl_2 have revealed[1] bands due to linearly adsorbed CO (2050 cm^{-1}) and 2-fold-bridged (B_2) CO (1880 cm^{-1}). Bands assigned to linear (2062 cm^{-1}) and 2-fold-bridge adsorbed CO (1941 cm^{-1}) were also detected[2] in infrared studies of CO adsorbed on palladium colloids in methylcyclohexane media. Infrared spectra of CO adsorbed on aqueous platinum colloids (hydrosols) feature[3] a band at 2065–2070 cm^{-1} due to CO adsorbed linearly on platinum while spectra of CO adsorbed[4] on palladium hydrosols reveal 2-fold bridged CO species (ca. 1950 cm^{-1}) in addition to linearly adsorbed CO species (ca. 2067 cm^{-1}). The band due to CO adsorbed linearly on platinum (ca. 2070 cm^{-1}) has been used in recent studies of surface processes in platinum hydrosols. The effect of electrolytes,[5] aliphatic alcohols,[6] and pH

(1) Lewis, L. N.; Lewis, N. *J. Am. Chem. Soc.* **1986**, *108*, 7228.

(2) Bradley, J. S.; Millar, J.; Hill, E. W.; Melchior, M. *J. Chem. Soc., Chem. Commun.* **1990**, 705.

(3) Mucalo, M. R.; Cooney, R. P. *J. Chem. Soc., Chem. Commun.* **1989**, 94.

(4) Mucalo, M. R.; Cooney, R. P. *J. Chem. Soc., Faraday Trans.* **1991**, *87*, 1221.

(5) Mucalo, M. R.; Cooney, R. P. *Can J. Chem.* (R. N. Jones Special Issue), to appear November, 1991.

(6) Mucalo, M. R.; Cooney, R. P., submitted to *J. Chem. Soc., Faraday Trans.*, in press.

0897-4756/91/2803-1081$02.50/0